Low-Light Image Enhancement using Image-to-Frequency Filter Learning

Rayan Al Sobbahi[1] and Joe Tekli[1]

[1] Department of Electrical and Computer Engineering, Lebanese American University (LAU), 36 Byblos, Lebanon
rayan.alsobbahi@lau.edu; joe.tekli@lau.edu.lb

Abstract. Low-light image (LLI) enhancement techniques have recently demonstrated remarkable progress especially with the use of deep learning (DL) approaches. Yet most existing techniques adopt an image-to-image learning paradigm where DL model architectures are constrained due to latent image feature reconstruction. In this paper, we propose a new LLI enhancement solution titled LLHFNet (Low-light Homomorphic Filtering Network) which performs image-to-frequency filter learning. It is designed independently from custom DL architectures and can be seamlessly coupled with existing feature extractors like ResNet50 and VGG16. We have conducted a large battery of experiments using SICE and Pascal VOC datasets to evaluate LLHFNet 's enhancement quality. Our solution consistently ranks among the best existing image enhancement techniques and is able to robustly handle LLIs and normal-light images (NLIs).

Keywords: Image enhancement, Low-light Conditions, Deep Learning, Homomorphic Filtering.

1 Introduction

Modern artificial intelligence-based applications like autonomous spacecrafts, drones, autopilot car systems, robots, and security surveillance systems, among others, rely on visualizing and understanding outdoor environments. While these systems show good performance during normal and clear outdoor conditions, yet varying weather conditions and poor illumination might challenge their visual perception and compromise their performance [1] [2]. Low-light conditions account to a considerable time of our daily lives and can significantly affect the robustness of such systems and hinder their market deployment [1]. Hence, low-light image (LLI) enhancement has emerged as an image processing task that aims at illuminating LLIs and improving their visual quality.

LLI enhancement techniques have been largely investigated recently. Many traditional approaches use gamma correction methods [3], some rely on histogram equalization methods [4], while others follow the Retinex theory model [5]. More recently, Deep learning (DL) techniques have demonstrated better performance and efficiency compared with traditional methods [6] [7]. Yet most of these models the image-to-image learning paradigm where the deep network architecture is constrained to produce an output image through latent feature reconstruction.

In this work, we introduce a novel LLI enhancement model titled LLHFNet (Low-light Homomorphic Filtering Network) based on image-to-frequency filter learning. Our approach aims at learning two homomorphic filter parameters, which are consequently applied on the input LLI to perform enhancement. This removes the constraints of performing full image reconstruction, while designing the DL model to solely focus on the image enhancement task. LLHFNet is independent from any specific architecture and can be seamlessly coupled with typical feature extractors utilized with existing classification models including ResNet50 [8], VGG16 [9], and MobileNetv2 [10], among others. We perform a battery of experiments to evaluate the performance of our approach. Results show improved results compared with recent LLI enhancement models, where our solution is able to robustly handle LLIs and normal-light images (NLIs).

Section 2 provides a review of the related works. Section 3 explains preliminaries on homomorphic filtering, Section 4 describes our LLI enhancement model. Section 5 describes our experimental evaluation and results, before concluding in Section 6.

2 Related Works

Traditional LLI enhancement techniques rely on mathematical or algorithmic models to perform the enhancement task. Many approaches use gamma correction methods [3], some rely on histogram equalization methods [4], while others follow the Retinex theory model [5] or utilize homomorphic filtering (HF) to perform image enhancement [11] [12]. In contrast with traditional approaches, Deep Learning (DL) techniques are essentially data-driven, where training datasets of LLIs and NLIs are used to drive the learning process. They have gained great attention in the past few years as the most effective solutions to perform LLI enhancement, outperforming many traditional methods based on histogram equalization, e.g., [4] [13] [14] and Retinex theory, e.g., [5] [15] [16] [17]. LLNet [6] is one of the first DL approaches for LLI enhancement. Its architecture is based on a stacked-sparse denoising autoencoder (SSDA) made of three denoising autoencoder layers comprising hidden units with no use of convolutional layers. In [18] authors introduce RetinexNet consisting of two subnetworks: i) DecomNet which learns the Retinex decomposition of the image into its reflectance and illumination components, and ii) EnhanceNet which uses a dedicated encoder-decoder structure to perform illumination adjustment and enhancement. In [19], the authors introduce GLADNET made of a global illumination estimation step, using an encoder-decoder structure followed by a reconstruction step through a series of convolutional layers. In [20], the authors propose MBLLEN, a multi-branch network which extracts the LLI features at each of its 10 convolutional layers through a special feature extraction module, and then enhances the features at each layer using an encoder-decoder network. The authors in [21] propose a DeepUPE to perform an image-to-illumination map learning. It consists of an encoder network based on a pre-trained VGG16 model [9], followed by a bilateral grid based up-sampling step to produce the image's full resolution illumination map, which is used to enhance the image based on the Retinex model. The authors in [22] introduce EnlightenGAN, an unsupervised generative adversarial network (GAN) approach based on attention guided U-Net [23] as its generator backbone, in addition to a global relativistic discriminator [24], and a local discriminator to handle spatially varying light conditions in the image. A recent approach in [25] proposes ZeroDCE, a zero reference deep curve estimation model which does not require any paired or unpaired training data. The authors reformulate the LLI enhancement task: from image-to-image learning into image-to-light curve learning. The light enhancement curves are estimated for each pixel using a lightweight deep curve estimation network (DCE-Net) thus resulting in an output with the same size of the input image.

DL LLI enhancement techniques are designed based on carefully curated architectures usually embodied within encoder-decoder networks to reconstruct latent features back to the image domain. In contrast, we introduce a novel LLI enhancement solution which performs image-to-frequency filter learning using Homomorphic Filtering (HF), focusing solely on the enhancement task independently of any specific DL architecture.

3 Preliminaries on Homomorphic Filtering

LLI enhancement models based on HF adopt the Retinex model representation of an image as a combination of illumination and reflective components. HF aims at converting the illumination and reflectance components which combine multiplicatively, into an additive form in the logarithmic domain [26]. The additive components are separated linearly in the Fourier transform frequency domain in which high-frequency components are associated with reflectance while low-frequency components correspond to illumination. A high-pass filter is used to suppress low frequencies and amplify high frequencies [26]. Figure 1 depicts the flow of the HF algorithm adopted in our approach.

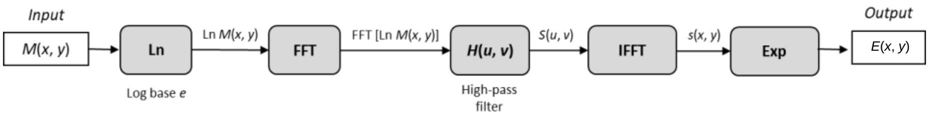

Fig. 1. HF algorithm flow (adapted based on [26]).

Step 0. The algorithm accepts as input an image following the Retinex Model:

$$M(x, y) = I(x, y) \times R(x, y) \tag{1}$$

where $M(x, y)$ is the original image, $I(x, y)$ is the illumination component, and $R(x, y)$ is the reflectance component.

Step 1. The logarithm of both sides of the Retinex model is taken to convert the illumination and reflective components from multiplicative form to additive form:

$$\ln M(x, y) = \ln I(x, y) + \ln R(x, y) \tag{2}$$

Step 2. The fast Fourier transform is applied to convert the image from the spatial domain to the frequency domain:

$$M(u, v) = I(u, v) + R(u, v) \tag{3}$$

where $M(u, v)$, $I(u, v)$ and $R(u, v)$ are the Fourier transforms of $M(x, y)$, $I(x, y)$ and $R(x, y)$ respectively. Note that $I(u, v)$ is mainly concentrated in the low frequency range while $R(u, v)$ is concentrated in the high frequency range.

Step 3. An appropriate high-pass filter with transfer function $H(u,v)$ is applied to perform the enhancement:

$$S(u,v) = H(u,v) \times M(u,v) \; = H(u,v)I(u,v) + H(u,v)R(u,v) \tag{4}$$

Step 4. The inverse Fourier transform is applied to transform the image from the frequency domain to the spatial domain. Let $s(x,y)$ be the inverse Fourier transform of $S(u,v)$, then the inverse Fourier transform of Formula 4 becomes:

$$s(x,y) = IFFT\big(H(u,v)I(u,v)\big) + IFFT\big(H(u,v)R(u,v)\big) = h_I(x,y) + \; h_R(x,y) \tag{5}$$

Step 5. Finally, the exponential operation is applied on Formula 5 to obtain the enhanced image denoted by $E(x,y)$:

$$E(x,y) = \exp[s(x,y)] = \exp[h_I(x,y)] \exp[h_R(x,y)] \tag{6}$$

4 LLI Enhancement Model

We design a new model titled LLHFNet (Low-light Homomorphic Filtering Network) which performs image-to-frequency filter learning instead of the typical image-to-image learning paradigm adopted by most existing solutions. The overall model architecture is depicted in Figure 2. It is based on HF where a special filter of two parameters is devised to filter the image frequency components in the Fourier transform domain. The two parameters are estimated using a typical DL-based feature extractor utilized in classification models. We describe the main components of our model including: i) enhancement filter design, ii) DL network architecture, and iii) loss function.

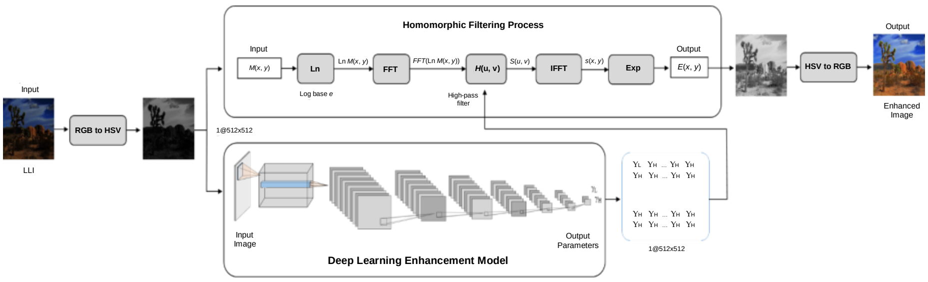

Fig. 2. LLHFNet image enhancement framework.

4.1 Enhancement Filter Design

A core part of the HF algorithm is the frequency filtering transform $H(u,v)$. In our design, we aim to produce a simple and effective filter transform that can be easily learned by the enhancement network. Here, the Fourier transform of the original image, i.e., $M(u,v)$ at (0,0), represents its DC-term[1] which corresponds to its average brightness in the spatial domain [27]. We make two interesting observations: i) $M(0,0)$ with LLIs is a large negative value reflecting the low brightness of these images, whereas ii)

[1] The DC-term is the 0 Hz term and is equivalent to the average of all the samples in the sampling window.

$M(0,0)$ for NLIs is either a small negative value or a positive value reflecting the normal brightness of these images. Based on the latter observations, we assume that brightness can be enhanced by increasing $M(0,0)$. We define our enhancement filter:

$$H(u,v) = \begin{cases} \gamma_L & (0,0) \\ \gamma_H & otherwise \end{cases} \tag{7}$$

where $\gamma_L \in [0,1]$ denotes the lightness parameter associated with low-frequency components and is placed at $H(0,0)$, and $\gamma_H \in [0,1]$ denotes the sharpness parameter associated with the remaining higher-frequency components of $M(u,v)$ corresponding to the image variations. The filter's behavior can be described as follows: i) the smaller (larger) the value of parameter γ_L, the higher (lower) the brightness level of the image, ii) the larger (smaller) the value of γ_H, the sharper (blurrier) the contents of the image.

We run the HF algorithm by applying our enhancement filter on the Value channel of the HSV (Hue-Saturation-Value) color domain, instead of using the Red, Green, and Blue channels of the RGB domain. We make this choice for the following reasons: i) it is more efficient to apply the Fourier transform and its inverse on one channel only instead of three, ii) the Value channel in HSV describes the lightness of the image which we aim to improve; while Hue and Saturation remain unchanged, and iii) HSV allows more simplicity with only two required parameters, compared with the RGB domain which may require two parameters for each of its channels to achieve good quality.

LLI | Enhanced Image ($\gamma_L = 0.35,\ \gamma_H = 0.45$) | LLI | Enhanced Image ($\gamma_L = 0.60, \gamma_H = 0.70$)

a. LLI with low exposure and the enhanced image

b. LLI with medium exposure and the enhanced image

Fig. 3. LLIs with from the SICE dataset [28] and their enhanced counterparts.

Figure 3 provides two examples highlighting the behavior of our enhancement filter with different exposure levels. On the one hand, Figure 3.a presents a LLI with a low exposure level, requiring parameter values <0.5 ($\gamma_L = 0.35$, $\gamma_H = 0.45$, cf. Formula 7) to produce a visually pleasing enhanced image with minimal artifacts. On the other hand, Figure 3.b presents a LLI with a medium exposure level, requiring relatively higher parameter values ($\gamma_L = 0.60$, $\gamma_H = 0.70$) to perform a minimal enhancement while avoiding overexposure. Here, there is a need to identify and fine-tune the parametric values of the filter function in order to maximize image enhancement quality. So, we develop a DL network model which can powerfully and efficiently extract high-level features from input images and allow estimating the values of parameters γ_L and γ_H while handling different input exposure levels.

4.2 Deep Learner Network Architecture

Our DL network architecture is depicted in Figure 4. It consists of two main parts: i) feature extractor, and ii) enhancement head. The *feature extractor* is responsible for extracting high-level features from the input images. Our solution allows the usage of any feature extractor network (e.g., VGG16 [9], ResNet50 [8], MobileNetv2 [10], SqueezeNet [29], among others) to perform the image-to-filter mapping, which comes down to estimating filter parameters γ_L and γ_H. We modify the first layer of the extractor to accept as input the Value channel of the image represented in the HSV domain.

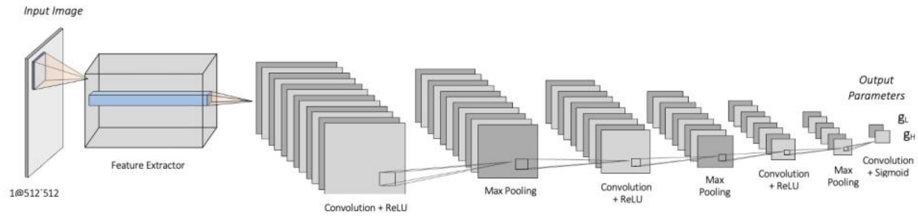

Fig. 4. DL enhancement model network architecture.

The *enhancement head* consists of four convolutional layers followed by ReLU activation and max pooling layers, allowing to downsize the feature maps obtained from the feature extractor. The last convolutional layer is followed by an adaptive average pooling layer to resize the network output to size 1x2x1, and then a Sigmoid activation function to limit the 2 output values representing γ_L and γ_H to the range [0,1], following our enhancement filter definition described in the previous section.

4.3 Enhancement Loss Function

The loss function is a major element of the LLI enhancement model and drives the entire learning process. In our approach, we adopt a supervised training setting in which reference-based loss functions are needed. We rely on Multi-scale Structural Similarity Index Measure (MS-SSIM) [30] for our loss function. MS-SSIM is an advanced version of SSIM which conducts assessment over multiple scales of the image. SSIM is widely used for image quality assessment as it can capture image contrast, structure, and illumination, e.g., [25] [21] [31], and is adopted as a loss function in many recent studies, e.g., [32] [33] [34]. Yet a recent empirical evaluation in [35] shows that quantitative image quality assessment metrics do not always correlate with the human perception of visual quality, due to the disparity between computational enhancement (done by the machine) and enhancement quality (perceived by humans). While the latter miscorrelation is difficult to evaluate through the loss function with existing image-to-image learning models, yet it is easier to monitor with our image-to-filter enhancement model (which seeks to learn two filter parameters only, rather than learning the image as a whole). In this context, a preliminary evaluation of our enhancement model shows two contradictory observations. On the one hand, an MS-SSIM based loss function may show a tendency to generate values for the lightness parameter γ_L which are greater than those of the sharpness parameter γ_H. This tends to produce enhanced images which are smoothed with distinctive color deviations, making them perceptually unpleasing. On the other hand, this tendency is encouraged by lower MS-SSIM loss values indicating that the metric is failing to properly quantify the quality of these enhanced images. To minimize the impact of this miscorrelation between qualitative perception and quantitative measure, we add a regularization term to the loss function, encouraging the learner model to generate values for γ_H which are greater than γ_L while reducing the overall loss value. More formally:

$$\text{enhLoss}(I_{\text{Enhanced}}, I_{\text{NLI}}) = 1\text{-MS\_SSIM}(I_{\text{Enhanced}}, I_{\text{NLI}}) + \alpha \times \ell \tag{8}$$

where *enhLoss* designates the enhancement loss function, $I_{Enhanced}$ is the enhanced image, I_{NLI} is the normal light image, $\ell = \gamma_L - \gamma_H$ is the regularization term, $\alpha >= 0$ is a linear weight parameter highlighting the impact of regularization on overall loss. Our empirical evaluation shows that values of α ranging between $[0.05, 0.1]$ produce satisfactory LLI enhancement results (in our experiments, we use $\alpha = 0.08$).

5 Experimental Evaluation

We perform an image quality assessment that aims at evaluating whether an image is visually pleasing and how it is visually perceived. We conduct both quantitative and qualitative evaluations, by evaluating the visual quality achieved by 5 prominent enhancement models (2 traditional solutions: SRIE [17] and LIME [15], and 3 DL-based solutions: ZeroDCE[2] [25], EnlightenGAN[3] [22] and DeepUPE[4] [21]). We compare the models with LLHFNet[5] implemented using PyTorch on a P100 Tesla Nvidia GPU, with a batch size of 8. We utilize an Adam optimizer with default parameters and a reduce-on-plateau decay-learning rate with an initial value of 1e-4 for network optimization. Our prototype implementation and experimental data are available online[5].

5.1 Experimental Data

We use the well-known SICE dataset [28] to conduct our training and testing experiments. We adopt two subsets for: i) training and ii) testing. The training subset consists of 2,150 image pairs from Part 1 of SICE, excluding extremely underexposed and overexposed images (which are difficult to handle and may tend to disrupt the training process). We resize all the training images to 512x512, and perform cross validation where 1700 pairs (i.e., 80%) are used for model learning and 450 pairs (i.e., 20%) are used for model evaluation. Although the training dataset seems relatively small, yet our enhancement model does not require huge training data since it relies on powerful pre-trained feature extractors for its backbone. In this experiment, we utilize five pre-trained extractors including VGG16 [9], ResNet50 [8], MobileNetv2 [10], SqueezeNet [29] and DenseNet [36]. The testing subset consists of 767 paired LLIs/NLIs collected from

[2] https://github.com/Li-Chongyi/Zero-DCE
[3] https://github.com/TAMU-VITA/EnlightenGAN
[4] https://github.com/wangruixing/DeepUPE
[5] https://github.com/rayanalsubbahi/LLHFNet

Part 2 of the SICE dataset [28] and resized to 1200x900x3 following the same approach adopted in [25] to perform our empirical evaluations. We additionally employ 3,000 images for testing from the well-known Pascal VOC 2007 dataset [37] and synthetically generate LLIs considering five different exposure levels using gamma correction with gamma values {4.5, 3.5, 2.5} corresponding to low-exposure levels, and gamma values {0.5, 0.8} corresponding to high-exposure levels. The subset is divided equally among the used (Υ corrected) exposure levels and all images are resized to 512x512.

5.2 Quantitative Evaluation Results

We run the enhancement models against three objective metrics commonly used in the literature: Structural Similarity index (SSIM) [38], Peak Signal to Noise Ratio (PSNR), and Mean Absolute Error (MAE). Table 1 shows quantitative IQA results comparing LLHFNet with its prominent counterparts, applied on SICE and Pascal VOC 2007 testing subsets. Our solution produces the best PSNR and MAE average scores, and the second best scores following SSIM on SICE while it ranks as the best following all three metrics on Pascal VOC 2007. Table 2 provides the average scores of LLHFNet using different feature extractors, including: ResNet50, MobileNetv2, VGG16, DenseNet, and SqueezeNet. MobileNetv2 and VGG16 produce some of the best average scores across all evaluation metrics using SICE subset. This is probably due to their dense architectures. ResNet50 shows second best result for all metrics on Pascal VOC 2007 indicating the effectiveness of the residual architecture in learning the filter parameters. SqueezeNet produces the worst results across all evaluation metrics, which is probably due to its lightweight architecture. Yet all LLHFNet variants show consistently competitive results when compared with the enhancement solutions in Table 1.

Table 1. Comparing the quality of existing LLI enhancement models. LLHFNet uses MobileNetv2 [10] as its feature extractor.

	a. SICE dataset			**b.** Pascal VOC dataset		
Model	SSIM ↑	PSNR ↑	MAE ↓	SSIM ↑	PSNR ↑	MAE ↓
LLHFNet	**0.58**	**16.89**	**94.99**	**0.734**	**15.77**	**117.07**
ZeroDCE	**0.59**	**16.57**	**98.78**	0.67	**14.96**	**139.05**
EnlightenGAN	**0.59**	16.21	102.78	0.6284	13.63	152.32
DeepUPE	0.49	13.52	142.01	**0.730**	14.30	143.89
LIME	0.57	16.17	108.12	0.6286	13.33	159.68
SRIE	0.54	14.41	127.08	0.629	13.50	154.69

Table 2. Comparing different feature extractors used with LLHFNet.

	a. SICE dataset			**b.** Pascal VOC dataset		
Feature Extractor	SSIM ↑	PSNR ↑	MAE ↓	SSIM ↑	PSNR ↑	MAE ↓
MobileNetv2	**0.583**	**16.896**	**94.992**	**0.734**	**15.775**	**117.078**
VGG16	**0.582**	**16.897**	**94.064**	0.728	15.590	121.214
ResNet50	0.577	16.686	96.152	**0.731**	**15.696**	**119.922**
DenseNet	0.576	16.716	97.253	0.730	15.563	120.855
SqueezeNet	0.575	16.593	99.129	0.726	15.442	122.063

Results in this experiment show that LLHFNet can be effectively used with different feature extractors, making it independent of any specific architecture.

5.3 Qualitative Evaluation Results

In addition to the quantitative evaluation, we also perform a qualitative evaluation to assess the human visual perception of images enhanced by our model and its five counterparts considered in this experiment. We randomly select 20 images from the SICE testing subset, and display the reference input LLI and the enhanced image side by side in a dedicated online survey[6]. Responders are asked to rate each image considering three visual IQA criteria including: i) level of exposure (over/under-exposed regions), ii) color deviations, and iii) overall beauty of the image. A total of 76 testers (senior computer engineering and master's students) were invited to contribute in the experiment, and independently rate every enhancement model on an integer scale from 1 to 10 (i.e., worst to best). We also deal with inconsistencies in image ratings by computing the average score for every image, and then eliminating ratings which have an extreme deviation from the average (e.g., ratings which are extremely low/high for images deemed visually pleasing/unpleasing). A total of at least 1200 responses were collected for each model, with every image receiving 60 rating scores. The ratings are aggregated for every enhancement model to evaluate its overall perceptual quality. Results are provided in Figure 5, and sample LLIs and enhanced images are shown in Figure 6.

Results in Figure 5 show that LLHFNet ranks second best among the five compared models, and is thus favored by human testers. Sample LLIs in Figure 6 show that LLHFNet produces visually pleasing enhanced images with minimal artifacts. In the first image (Figure 6.a), our model is able to uncover the dark regions of the fence and is able to effectively restore the green colors of the trees. In the second image (Figure 6.b), our model properly restores the colors of the trees, grass, and white clouds without overexposing them (compared with EnlightenGAN where the clouds are overexposed, and ZeroDCE and SRIE where the cloud colors and overall image colors deviate into blue). In the third image (Figure 6.c), our model shows a good illumination level and produces results comparable with to ZeroDCE and SRIE. The reader can refer to [39] for a detailed description of the experimental results, as well as the whole framework.

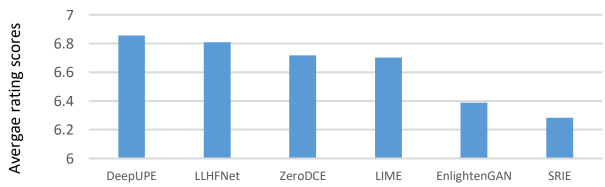

Fig. 5. Average user ratings for the enhancement models ranked from best to worst.

[6] https://forms.gle/FrjzGAZXpyKqGRnw9

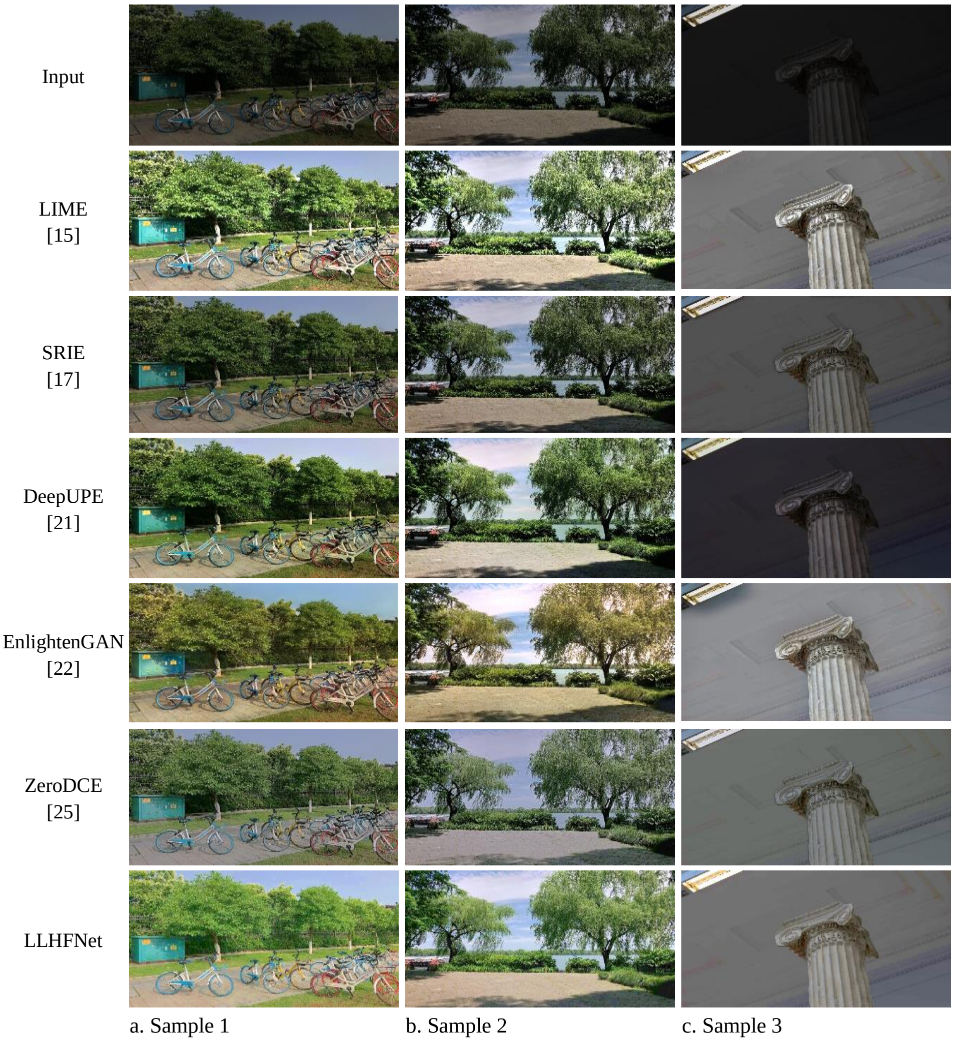

Fig. 6. Visual comparison of sample LLIs from SICE Part 2 [28] and their enhanced versions.

6 Conclusion

In this paper, we introduce a new LLI enhancement solution titled LLHFNet (Low-light Homomorphic Filtering Network) based on image-to-frequency filter learning. The network is designed independently from a custom architecture and can use many feature extractors commonly adopted in object classification. Experimental results show improved enhancement quality on LLIs, and is ranked among the best enhancement models compared with recent solutions. We are currently conducting an empirical study to evaluate the performance of our solution on extremely LLIs. In the near future, we aim to integrate and evaluate our enhancement model in high-level tasks like object detection [40], image semantization [41], localization and tracking [42, 43], and multi-label image recognition [44].

References

1. Yang, W., et al.: Advancing Image Understanding in Poor Visibility Environments: A Collective Benchmark Study. IEEE Trans. Image Process. (IEEE TIP), 29, 5737-5752 (2020).
2. Scheirer, W., et al.: Bridging the Gap Between Computational Photography and Visual Recognition. IEEE TPAMI. 1-1 (2020).
3. Zhi, N., et al..: An Enhancement Algorithm for Coal Mine Low Illumination Images based on Bi-Gamma Function. J. Liaoning Tech. Univ. 37(1), 191-197 (2018).
4. Kansal, S., et al.: Image Contrast Enhancement Using Unsharp Masking and Histogram Equalization. Multimedia Tools Appl. 77(20), 26919–26938 (2018).
5. Ren, X., et al.: LR3M: Robust Low-light Enhancement via Low-rank Regularized Retinex Model. IEEE Trans. Image Process. 29, 5862-5876 (2020).
6. Lore, K. G., et al., LLNet: A Deep Autoencoder Approach to Natural LLI Enhancement. Pattern Recognit. 61, 650-662 (2017).
7. Li, C., et al.: LightenNet: A Convolutional Neural Network for Weakly Illuminated Image Enhancement. Pattern Recognit. Lett. 104, 15-22 (2018).
8. He, K., et al., Deep Residual Learning for Image Recognition. IEEE CVPR Conf., pp. 770-778. IEEE Press (2016).
9. Simonyan K. et al., Very Deep Convolutional Networks for Large-Scale Image Recognition. In: arXiv:1409.1556 (2015).
10. Sandler, M., et al.: MobileNetV2: Inverted Residuals and Linear Bottlenecks. IEEE CVPR, 4510-4520 (2018).
11. Zhang, C., et al.: Color Image Enhancement based on Local Spatial Homomorphic Filtering and Gradient Domain Variance Guided Image Filtering. J. Electron. Imaging. 27(6) (2018).
12. Han, L., et al.: Using HSV Space Real-color Image Enhanced by Homomorphic Filter in Two Channels. Comput. Eng. Appl. 45(27), 18-20 (2009).
13. Abdullah-Al-Wadud, et al.: A Dynamic Histogram Equalization for Image Contrast Enhancement. IEEE Trans. Consum. Electron. 53(2), 593-600 (2007).
14. Gu, K.: Automatic Contrast Enhancement Technology with Saliency Preservation. IEEE TCSVT, 25(9), 1480-1494 (2015).
15. Li, L. et al., A Low-light Image Enhancement Method for both Denoising and Contrast Enlarging. In: IEEE Int. Conf. Image Process. (ICIP), pp. 3730–3734. IEEE Press (2015).
16. Li, M., et al.: Structure-revealing Low-light Image Enhancement via Robust Retinex Model. IEEE Trans. Image Process. 27(6), 2828–2841 (2018).
17. Fu, X., et al.: A Weighted Variational Model for Simultaneous Reflectance and Illumination Estimation. 2016 IEEE Conf. Comput. Vis. Pattern Recogn., pp. 2782-2790, (2016).
18. Wei, C. et al.: Deep Retinex Decomposition for Low-light Enhancement. In: Inter. BMVC Conf., pp. 1-12 (2018).
19. Wang, W., et al.: GLADNet: Low-light Enhancement Network with Global Awareness. IEEE Autom. Face Gesture Recognit., pp. 751-755. IEEE Press, New York (2018).
20. Lv, F. et al.: MBLLEN: Low-light Image/Video Enhancement Using CNNs. In: Proc. Brit. Mach. Vis. Conf. pp. 1-13 (2018).
21. Wang, R., et al.: Underexposed Photo Enhancement Using Deep Illumination Estimation. IEEE CVPR Conf., 6842–6850 (2019).

22. Jiang, Y., et al.: EnlightenGAN: Deep Light Enhancement without Paired Supervision. IEEE TIP, 30, 2340-2349 (2021).
23. Ronneberger O., et al.: U-Net: Convolutional Networks for Biomedical Image Segmentation. arXiv:1505.04597 (2015).
24. Jolicoeur-Martineau, A.: The Relativistic Discriminator: A Key Element Missing from Standard GAN. In: arXiv:1807.00734 (2018) http://arxiv.org/abs/1807.00734.
25. Guo, C., et al.: Zero-Reference Deep Curve Estimation for Low-Light Image Enhancement. IEEE CVPR, 1777-1786 (2020).
26. Wang, W., et al.: An Experiment-based Review of LLI Enhancement Methods. IEEE Access. 8, 87884-87917 (2020).
27. Gonzalez, C. and Woods, E.: Digital Image Processing. 4th ed. Pearson, NY (2018).
28. Cai, J., et al.: Learning a Deep Single Image Contrast Enhancer from Multi-exposure Images. IEEE TIP, 27(4):2049-2062 (2018).
29. Iandola, F. N.: Squeezenet: Alexnet-level Accuracy with 50x Fewer Parameters and <0.5 mb Model Size. In: arXiv:1602.07360 (2016), Available: http://arxiv.org/abs/1602.07360.
30. Wang, Z., et al.: Multiscale Structural Similarity for Image Quality Assessment. In: 37th Asilomar Conf. Signals, Syst. Comput., pp. 1398-1402. IEEE Press (2003).
31. Ren, W., et al.: Low-Light Image Enhancement via a Deep Hybrid Network. IEEE Trans. Image Process. 28, 4364-4375 (2019).
32. Xiang Y., et al.: An Effective Network with ConvLSTM for Low-Light Image Enhancement. In Chinese Conf. Comput. Vis. Pattern Recognit. (PRCV), pp. 221-233 (2019).
33. Zhang, Y.: Kindling the Darkness: A Practical Low-light Image Enhancer. ACM MM Conf., pp. 1632–1640 (2019).
34. Shi, Y., et al.: Low-light Image Enhancement Algorithm Based on Retinex and Generative Adversarial Network. Computing Research Repository, CoRR 1906.06027 (2019).
35. Al Sobbahi, R. and Tekli, J.: Comparing Deep Learning Models for Low-light Image Enhancement and their Impact on Object Detection and Classification. Signal Process.: Image Comm. journal, (2022).
36. Huang, G., et al.: Densely Connected Convolutional Networks. IEEE CVPR Conf., pp. 4700-4708. IEEE Press (2017).
37. Everingham, M. et al.: Pascal Visual Object Classes (VOC) Challenge. Int. J. Comput. Vis. 88(2), 303-338 (2010).
38. Wang Z., et al.: Image Quality Assessment: From Error Visibility to Structural Similarity. IEEE Trans. Image Process. 13(4), 600-612 (2004).
39. Al Sobbahi, R. and Tekli, J.: Low-Light Homomorphic Filtering Network for Integrating Image Enhancement and Classification. Signal Process.: Image Comm., 100:116527 (2022).
40. Salem, C. et al.: An Image Processing and Genetic Algorithm-Based Approach for the Detection of Melanoma in Patients. Methods Inf. Med. 57(1): 74-80 (2018).
41. Salameh K., et al.:. SVG-to-RDF Image Semantization. Inter. Conf. on Similarity Search and Apps. (SISAP'14), pp. 214-228 (2014)
42. Ebrahimi, D. et al.: Autonomous UAV Trajectory for Localizing Ground Objects: A Reinforcement Learning Approach. IEEE Trans. Mobile Comput. 20(4): 1312-1324 (2021).
43. Samir M. et al.: Age of Information Aware Trajectory Planning of UAVs in Intelligent Transportation Systems: A Deep Learning Approach. IEEE Trans. Veh. Technol. 69(11): 12382-12395 (2020).
44. Laib L. et al.: A Probabilistic Topic Model for Event-based Image Classification and Multi-label Annotation, Signal Process.: Image Comm., 76: 283-294 (2019).